Pressure-induced decay of the Griffiths phase and accompanying exchange-bias collapse in $Gd_{0.5}Sr_{0.5}CoO_{3-\delta}$

I. Fita,[1,*] I. O. Troyanchuk,[2] T. Zajarniuk,[1] A. Wisniewski,[1] and R. Puzniak[1]
[1]*Institute of Physics, Polish Academy of Sciences, Aleja Lotnikow 32/46, PL-02668 Warsaw, Poland*
[2]*Scientific-Practical Materials Research Centre, NAS of Belarus, P. Brovka street 19, BY-220072 Minsk, Belarus*

(Received 9 April 2020; accepted 3 June 2020; published 25 June 2020)

The effect of pressure on both ferromagnetic (FM) cluster phase and the Griffiths phase (GP) was investigated in disordered cobaltite $Gd_{0.5}Sr_{0.5}CoO_{3-\delta}$, exhibiting low $T_C = 90$ K, high Griffiths temperature $T_G = 220$ K, and the exchange bias (EB) effect, which exists exotically inside GP. It was found that applied pressure leads to a decrease of T_C with a coefficient of $dT_C/dP = -1$ K/kbar and dramatically suppresses GP, resulting in a rapid decrease in T_G at a rate of $dT_G/dP = -3.6$ K/kbar. Similarly, the EB field does not change significantly in the FM phase but it promptly collapses with pressure in GP, e.g., the EB field decreases four times under 10 kbar at 140 K. It appears that external pressure effectively eliminates local structure deformations that are responsible for magnetically ordered clusters existing above T_C. It is suggested that the well-known pressure-induced transition from the high-spin Co^{3+} state to the low-spin state is mainly responsible for the observed decay of the Griffiths phase and simultaneous EB collapse, as well as, for a decrease in T_C under pressure in $Gd_{0.5}Sr_{0.5}CoO_{3-\delta}$.

DOI: 10.1103/PhysRevB.101.224433

An intrinsic electronic inhomogeneity is a very relevant feature of complex oxide compounds like manganites or cobaltites. They exhibit phase separation, i.e., a coexistence of different phases with variety of electronic, structural, and magnetic properties. The examples of such materials are: metallic ferromagnetic droplets in an insulating background or vice versa insulating droplets in a metallic ferromagnet. The length scales of these inhomogeneities range from nanometers to micrometers. Phase separation leads to many interesting properties of these compounds, among others to an appearance of exchange-bias (EB) effect. Ferromagnetic (FM) perovskite cobaltites $R_{1-x}M_xCoO_3$ ($R =$ rare earth metal, $M =$ Ca, Sr, Ba) exhibit additional exceptional physical properties, primarily due to the alternating spin states of the Co ion: low-spin (LS) $S = 0$, intermediate-spin (IS) $S = 1$, and high-spin (HS) $S = 2$, that can coexist in the crystal depending on doping, temperature, crystal structure deformations, and external pressure [1–5]. The coupling between the Co spin state and the lattice supports the magnetic phase separation, which manifests itself in the coexisting FM, spin glass (SG), and nonmagnetic nanoscale regions [6–8] and provides below T_C the FM cluster glassy behavior [8] and specific EB effect [9,10], which is emergent due to exchange interaction at the FM/SG interface [11–14]. A diversity of Co spin states can also favor the Griffiths phase (GP), representing short-range FM clusters embedded in a paramagnetic matrix that exhibit nonanalytical magnetic behavior between T_C and the Griffiths temperature T_G [15]. The quenched disorder in the structure, i.e., the presence of random local lattice distortions due to size mismatch of the dopant ions, is one of the main reasons for the formation of GP in perovskites [16]. Interestingly, the clear GP revealed by the downward deviation in the inverse susceptibility χ^{-1} from the Curie-Weiss (CW) law below T_G was found in $La_{1-x}Ca_xCoO_3$ cobaltites [17], in contrast to the non-Griffiths-like behavior (namely the upward deviation in χ^{-1} from the CW law) reported for Sr- and Ba-doped compounds [18,19]. The different behavior is probably due to the fact that the Co-Co interactions are antiferromagnetic (AFM) linked to HS Co^{3+} states in the crystals with expanded lattice, doped with larger Sr and Ba ions, while they are FM associated with the IS Co^{3+} states in the case of doping with Ca ion [4,20,21]. An exceptional situation was found in disordered $Gd_{0.5}Sr_{0.5}CoO_{3-\delta}$ in which the Griffiths phase, resulting from the replacement of the La ion by the smaller Gd ion, extends above T_C up to $T_G \sim 2T_C$. More interestingly, this GP demonstrates a noticeable EB effect, suggesting the coexistence of both FM and AFM nanoscale phases above T_C [22]. This is a reminiscent of the transition from the non-Griffiths-like behavior to the Griffiths phase, caused by a decrease in particle size reported in $La_{0.7}Sr_{0.3}CoO_3$ [23]. External pressure is also a tool that can change the magnetic state of cobaltites due to the well-known pressure-induced transition from the HS Co^{3+} state to the LS state [24]. In the present paper, we show that the applied pressure lowers T_C in $Gd_{0.5}Sr_{0.5}CoO_{3-\delta}$ and strongly suppresses GP, while the associated EB simultaneously collapses. We suggest that external pressure effectively eliminates local structure deformations responsible for the coexistence of both FM and AFM nanoclusters above T_C and the pressure-induced decrease in the Co^{3+} spin state plays an important role in this process.

The pressure study was performed on polycrystalline $Gd_{0.5}Sr_{0.5}CoO_{3-\delta}$ sample for which the simultaneous coexistence of both the Griffiths phase and exchange bias effect at temperatures above T_C was recently found [22], see also

*Corresponding author: ifita@ifpan.edu.pl

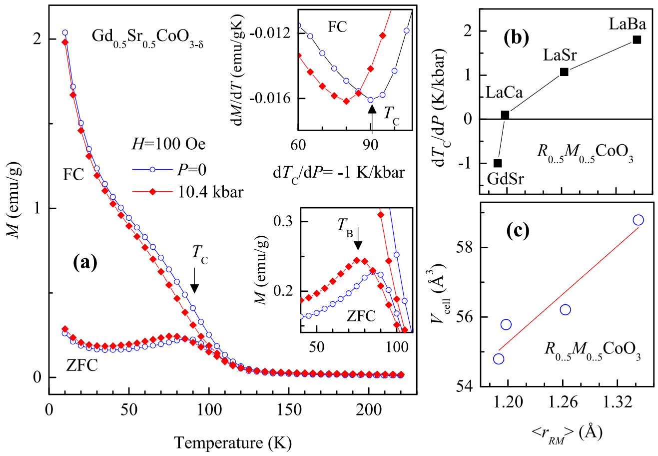

FIG. 1. (a) Temperature dependence of the ZFC and FC magnetization of $Gd_{0.5}Sr_{0.5}CoO_{3-\delta}$ measured in 100 Oe at ambient pressure and at $P = 10.4$ kbar. The upper inset shows pressure-induced shift in temperature of minimum of the derivative dM/dT, associated with T_C, and the lower inset shows a decrease of blocking temperature T_B under pressure. (b), (c) Change of sign in pressure coefficient dT_C/dP (b) and increase of the unit cell volume V_{cell} (c) with increasing average R-site cation radius in half-doped cobaltites $R_{0.5}M_{0.5}CoO_3$, where R = La, Gd, and M = Ca, Sr, Ba.

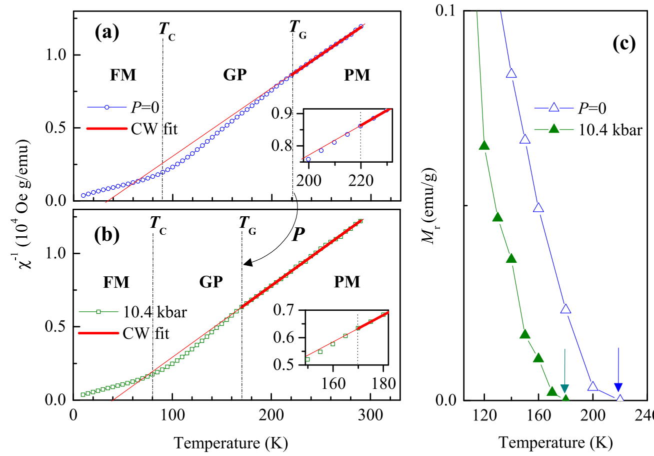

FIG. 2. The inverse dc susceptibility χ^{-1} of $Gd_{0.5}Sr_{0.5}CoO_{3-\delta}$ as function of temperature, measured in magnetic field of 10 kOe, at $P = 0$ (a) and under pressure of 10.4 kbar (b). The solid lines are CW fits accomplished for the PM state, and the insets show deviation from the CW law below the Griffiths temperature T_G. The Griffiths phase (GP) region, selected between temperatures T_C and T_G, collapses under pressure. (c) The remanent magnetization M_r, measured at $H = 0$ after FC with 15 kOe, shows a decrease of temperature at which FM clusters appear (indicated by arrows) under pressure.

Ref. [25] for details of the sample preparation and characterization. The dc magnetization measurements, such as temperature dependences recorded in fixed magnetic field and hysteresis loops at fixed temperature in both field cooling (FC) and zero field cooling (ZFC) modes, for the temperature range 10–290 K, in magnetic field up to 15 kOe, were performed using the Princeton Applied Research (Model 4500) vibrating sample magnetometer. Magnetization measurements under hydrostatic pressure up to 10.4 kbar were performed using a miniature container of CuBe with an inside diameter of 1.4 mm [26] exploiting the silicon oil as a pressure-transmitting medium. The pressure at low temperatures was determined by the known pressure dependence of the superconducting transition temperature of pure tin.

Figure 1 presents the temperature dependence of ZFC and FC magnetization of $Gd_{0.5}Sr_{0.5}CoO_{3-\delta}$ measured in 100 Oe at ambient pressure and at $P = 10.4$ kbar. Applied pressure leads to a decrease of both blocking temperature T_B and the Curie temperature T_C, see insets in Fig. 1, where T_B is the temperature of maximum in ZFC magnetization and T_C is defined as temperature of minimum in derivative dM_{FC}/dT. Obtained pressure coefficient $dT_C/dP = -1$ K/kbar is compared in Fig. 1(b) with those previously found for $La_{0.5}M_{0.5}CoO_3$ (M = Ca, Sr, Ba) half-doped cobaltites [27]: the coefficient dT_C/dP monotonically increases and changes sign with increasing average M-site cation radius (calculated for the ninefold oxygen coordination), and/or with increasing the unit cell volume [see Fig. 1(c)]. Very similar behavior has been observed previously for low-doped $La_{0.8}M_{0.2}CoO_3$ (M = Ca, Sr, Ba) cobaltites and was well described in terms of competing pressure-induced changes in the e_g-electron bandwidth W and crystal-field t_{2g}-e_g splitting energy Δ_{cf} [27]. In general, the T_C of doped cobaltites is determined by the competing bandwidth W and crystal-field energy Δ_{cf}, namely, it is proportional to the effective energy $(W/2 - \Delta_{cf} + J_{ex})$, which is a measure of the population of magnetic IS state [28]. Both energies, $W \sim \cos\omega(d_{\text{Co-O}})^{-3.5}$ and $\Delta_{cf} \sim (d_{\text{Co-O}})^{-5}$, always increase under pressure due to contraction of the Co-O bond length $d_{\text{Co-O}}$, as well as, of bending angle $\omega = (180^\circ - \langle\text{Co-O-Co}\rangle)/2$, while the Hund's coupling J_{ex} does not depend on pressure. It appears that the pressure coefficient dT_C/dP is strongly dependent on the Δ_{cf} to W ratio. It was calculated in Ref. [27], using typical bond length and bond angle compressibility data for cobaltites, that the dT_C/dP coefficient becomes negative when $\Delta_{cf}/W > 0.38$. It means that the population of nonmagnetic LS state increases and T_C lowers under pressure in compounds with narrow bandwidth W and small enough T_C. This requirement complies well with the values of $dT_C/dP = -1$ K/kbar and $T_C = 90$ K observed for $Gd_{0.5}Sr_{0.5}CoO_{3-\delta}$. In contrast, $La_{0.5}Sr_{0.5}CoO_3$ exhibits positive $dT_C/dP = +1.07$ K/kbar and high $T_C = 260$ K. This difference demonstrates the robust Gd for La substitution effect in Sr-doped cobaltites, leading to the narrow bandwidth W and large splitting energy Δ_{cf}, and, therefore, to the low T_C and negative coefficient dT_C/dP in $Gd_{0.5}Sr_{0.5}CoO_{3-\delta}$.

Figures 2(a) and 2(b) present the dc inverse susceptibility χ^{-1} as a function of temperature recorded in magnetic field of 10 kOe in the temperature range between 10 and 290 K at $P = 0$ (a) and under pressure of 10.4 kbar (b). The presented $\chi^{-1}(T)$ curves clearly reveal the Griffiths singularity in $Gd_{0.5}Sr_{0.5}CoO_{3-\delta}$ even if it is significantly suppressed by large applied field of 10 kOe, as compared to that measured with $H = 10$ Oe at $P = 0$, which was well described in Ref. [22] by the power law $\chi^{-1} \propto (T/T_C^R - 1)^{1-\lambda}$ proposed for the system of FM clusters with randomly distributed sizes embedded in the paramagnetic (PM) matrix [29,30]. Notice that, despite of large magnetization contribution from the PM phase, we

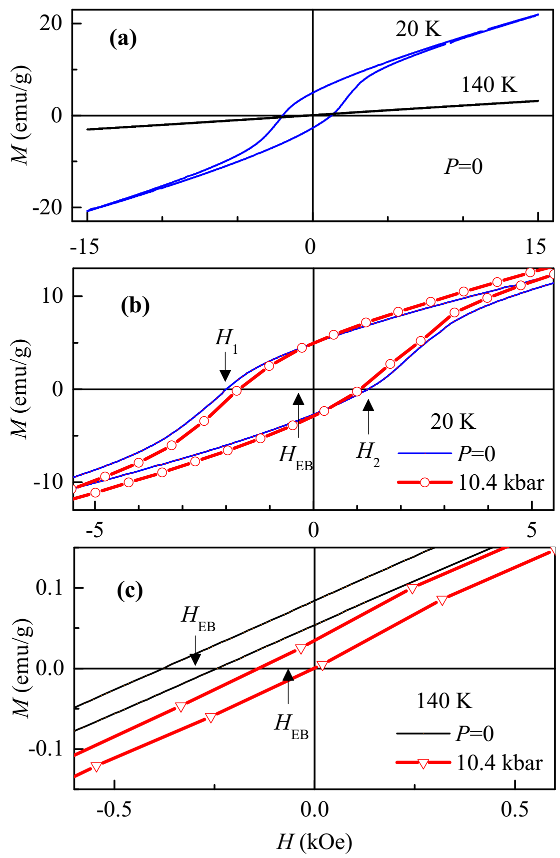

FIG. 3. Magnetization hysteresis loops of $Gd_{0.5}Sr_{0.5}CoO_{3-\delta}$, typical for FM phase ($T = 20$ K) and for the Griffiths phase ($T = 140$ K), measured with cooling field $H_{cool} = 15$ kOe at ambient pressure $P = 0$ (a). Loops measured at both $P = 0$ and $P = 10.4$ kbar at temperatures of 20 K (b) and 140 K (c), shown in the extended scale. Arrows indicate the negative H_1 and positive H_2 coercive fields (b) and a pressure-induced shift in EB field at 140 K (c).

used the high measuring field of 10 kOe providing precise χ data and allowing to fix precisely the temperature T_G below which χ^{-1} starts to deviate downward from the CW law [see insets in Figs. 2(a) and 2(b)]. It is demonstrated in Figs. 2(a) and 2(b) that the temperature region for which the CW law $\chi = C/(T - \theta)$ thoroughly obeys, extends under applied pressure, indicating the pressure-induced loss of the FM clusters and temperature T_G decreases significantly. Thus, the applied pressure extensively modifies the magnetic phase diagram of $Gd_{0.5}Sr_{0.5}CoO_{3-\delta}$, namely, the temperature region of pure PM phase expands under pressure while that of coexistence of GP and FM phases contracts. Note that observation of pressure-induced annihilation of the FM clusters in perovskite cobaltites is exclusive. This exceptional behavior is confirmed further by the pressure-dependent remanent magnetization M_r, measured at zero field after field cooling with $H = 15$ kOe accomplished at each temperature. It is demonstrated in Fig. 2(c) that M_r, which is a measure of the FM cluster-phase volume, disappears at about the same temperatures T_G that were determined from the χ^{-1} data, presented in Figs. 2(a) and 2(b) at $P = 0$ and under pressure of 10.4 kbar.

Useful information on pressure-induced changes in Co spin state is obtained from the analysis of CW linear behavior in the PM region above T_G. The CW fit [see the bold lines in Figs. 2(a) and 2(b)] gives the Curie constant C equal to 0.0214 emu K/g Oe at $P = 0$ and 0.0204 emu K/g Oe at 10.4 kbar, both obtained with 1% accuracy. Accordingly, the effective PM moment $p_{eff} = g\mu_B[S(S+1)]^{1/2}$ changes from 6.27 to 6.105 μ_B under 10.4 kbar pressure. The p_{eff} includes both Co and Gd^{3+} contributions, and we assume that the paramagnetic Gd^{3+} ions are free and have effective moment $p^{Gd}{}_{eff} = 7.8\,\mu_B$ (calculated for spin $S = 7/2$ and $g = 2$) which does not depend on pressure. After subtracting the Gd^{3+} contribution by means of relation: $p^{Co}{}_{eff} = [(p_{eff})^2 - 0.5(p^{Gd}{}_{eff})^2]^{1/2}$, one obtains that the effective Co moment $p^{Co}{}_{eff}$ diminishes its value from 2.96 μ_B (under ambient pressure) to 2.62 μ_B (under pressure of 10.4 kbar), while the average value of Co spin S_{av} reduces from 1.065 to 0.903. The result replicates the specific feature of cobaltites to change the Co^{3+} spin state from magnetic HS or IS states to the nonmagnetic LS state under pressure due to the contraction of bond length $d_{Co\text{-}O}$. This mechanism is understandable since the ionic radius of LS Co^{3+} (0.545 Å) is smaller than that of IS Co^{3+} (0.56 Å), and the difference is likely responsible for the pressure-induced decay of the FM clusters in $Gd_{0.5}Sr_{0.5}CoO_{3-\delta}$.

In order to obtain further insight into nature of pressure-induced conversion of GP to the pure PM phase, the effect of pressure on EB, which is a prominent feature of GP in $Gd_{0.5}Sr_{0.5}CoO_{3-\delta}$, signifying the coexistence of short-range FM and AFM cluster phases in the temperature range between T_C and T_G, was investigated. Figure 3 shows the magnetization hysteresis loops representative for the FM cluster phase ($T = 20$ K) and GP ($T = 140$ K), all measured with cooling field 15 kOe at $P = 0$ and under pressure of 10.4 kbar. One can noticed the shift of hysteresis loop center for both FM phase and GP, defined as negative EB field $H_{EB} = (H_1 + H_2)/2$, where H_1 and H_2 are the negative and positive coercive fields, respectively. Figure 4(a) presents the H_{EB} vs temperature curves at several pressures. They show that applied external pressure does not change significantly the field H_{EB} in the FM phase but it dramatically suppresses H_{EB} in the GP. Notably, EB vanishes closely at the same temperature T_G, at which the $\chi^{-1}(T)$ dependence is found to deviate from the CW law [see Figs. 2(a) and 2(b)]. This proves that EB is inherent to GP of $Gd_{0.5}Sr_{0.5}CoO_{3-\delta}$, hence, GP may be detected in the sample by measuring EB. With increasing pressure, the temperature range of EB existence progressively contracts and the field H_{EB} weakens. It results that T_G decreases linearly with pressure with coefficient $dT_G/dP = -3.6$ K/kbar [see Fig. 4(b)]. At an applied pressure of 10.4 kbar, the field H_{EB} decreases by more than four times at $T = 140$ K and completely disappears at temperatures $T \geqslant 170$ K. In contrast, the average coercive field H_C, defined as $H_C = (H_2 - H_1)/2$ (it is a half width of the loop), does not change visibly [see Fig. 4(c)]. Contrasting H_C and H_{EB} vs P dependences may provide insight into the nature of FM clusters in GP. For small single-domain FM nanoparticles, the coercive field H_C is expected to decrease with reducing particle diameter D according to the law $H_C \propto 1 - (D_S/D)^{3/2}$, where D_S is the particle diameter at which the superparamagnetic limit ($H_C = 0$) is reached [31]. Such behavior has been well verified for both manganite [32] and cobaltite [33] FM nanoparticles with size $D < 20$ nm. Since the H_C value at $T = 140$ K remains almost unchanged under

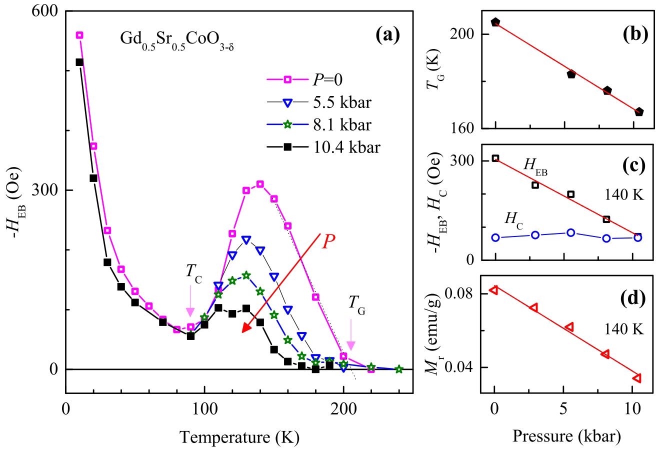

FIG. 4. (a) Exchange-bias field H_{EB} as function of temperature at several pressures. The nonmonotonic H_{EB} vs T dependence is characteristic of GP. (b) Linear decrease of the Griffiths temperature T_{G} with pressure with coefficient $dT_{\mathrm{G}}/dP = -3.6\,\mathrm{K/kbar}$. For both H_{EB} (c) and remanent magnetization M_{r} (d) a linear decrease with increasing pressure is observed at $T = 140\,\mathrm{K}$, while the coercive field H_{C} is invariable (c).

pressure [see Fig. 4(c)], one can expect that the FM cluster size does not change. This is surprising since the EB field is known to depend strongly on the cluster size in phase-separated FM/AFM systems. In order to clarify this issue, we investigated the field H_{EB} as a function of cooling field H_{cool} at $T = 140$ K at several pressures, see Fig. 5(a). One can notice that despite a strong suppression of H_{EB} under pressure, the character of the $H_{\mathrm{EB}}(H_{\mathrm{cool}})$ dependence exhibits the same tendency. Basing on the H_{EB} vs H_{cool} dependence, the average cluster size can be estimated using the model considering a system of single-domain FM clusters embedded in the AFM matrix [34]:

$$H_{\mathrm{EB}} \propto J[(J\mu_0/(g\mu_{\mathrm{B}})^2)\mathrm{L}(\mu H_{\mathrm{cool}}/k_{\mathrm{B}}T_{\mathrm{f}}) + H_{\mathrm{cool}}], \tag{1}$$

where J is the interface exchange constant, $g = 2$ is the Lande factor, μ_{B} is the Bohr magneton, L denotes the Langevin function, $\mu_0 = 2\mu_{\mathrm{B}}$ is the magnetic moment per Co^{3+} ion with spin $S = 1$, $\mu = N\mu_0$ is the magnetic moment of the FM clusters with N number of spins within the cluster, and T_{f} is the freezing temperature below which both coercive and EB fields appear. Notice, this model has been successfully used for evaluation of the FM cluster size in a variety of exchange-biased manganites and cobaltites [35]. The solid lines in Fig. 5(a) are the best fits with Eq. (1), obtained with the values of fitting parameters N and J calculated for the each value of applied pressure. Based on the obtained values of N and taking into account that the freezing temperature T_{f} here is in fact the pressure-dependent temperature T_{G} [see Fig. 4(b)], the FM cluster size D at each applied pressure was estimated. The above analysis shows that both cluster size $D \approx 6.5$ nm and interface exchange interaction $J/g\mu_{\mathrm{B}} \approx 50$ kOe are practically unchanged under pressure up to 10 kbar [see Figs. 5(b) and 5(c)]. This conclusion leads to difficulty in interpretation of observed fourfold reduction in the field H_{EB} under pressure of 10 kbar at 140 K, presented in Fig. 4(c). Previously, the EB effect in GP of $Gd_{0.5}Sr_{0.5}CoO_{3\text{-}\delta}$ has been interpreted within the simple Meiklejohn-Bean (MB) model regarding a system of small isolated FM clusters embedded in the AFM matrix [22]. Within MB model the H_{EB} is determined by the ratio of the interfacial exchange energy J to the product of magnetization M_{FM} and thickness t_{FM} of the FM layers and depends on both AFM anisotropy K_{AFM} and thickness of the AFM layers t_{AFM} [36]:

$$H_{\mathrm{EB}} = \begin{matrix} (-J/M_{\mathrm{FM}}t_{\mathrm{FM}})(1 - 1/4R^2)^{1/2} & \text{for } R \geqslant 1 \\ 0 & \text{for } R < 1 \end{matrix}, \tag{2}$$

where the parameter $R \equiv K_{\mathrm{AFM}}t_{\mathrm{AFM}}/J$ determines the region of existing EB in the system, namely, the EB exists only when $R \geqslant 1$, i.e., when the AFM anisotropy energy $K_{\mathrm{AFM}}\,t_{\mathrm{AFM}}$ is large enough, and $H_{\mathrm{EB}} = 0$ when $R < 1$. In the case of a system comprising the FM clusters of size D, distributed in an AFM matrix, one needs to replace t_{FM} by $D/6$. It appears that Eq. (2) is not capable to explain the strong pressure-induced decrease of field H_{EB} observed at 140 K in $Gd_{0.5}Sr_{0.5}CoO_{3\text{-}\delta}$, since the ratio J/D is nearly unchanged under pressure [see Fig. 5(d)], while the term $(1 - 1/4R^2)^{1/2}$ can only decline by 15% when R varies between large values and 1. Most likely, the inconsistency arises since the structure of the coexisting FM and AFM phases in GP is actually more complex than that which is considered in the above model. An additional difficulty in interpretation of peculiar pressure-dependent EB appears because the number of FM clusters in the system varies under pressure. Actually, it is puzzling why some FM clusters annihilate under pressure while others do not change the size. If so, the concentration of FM clusters should decrease by more than two times upon application a pressure of 10 kbar at 140 K, as follows from the remanent magnetization M_{r} data shown in Fig. 4(d). Such a process is consistent with the observed pressure-induced conversion of the GP to pure PM phase.

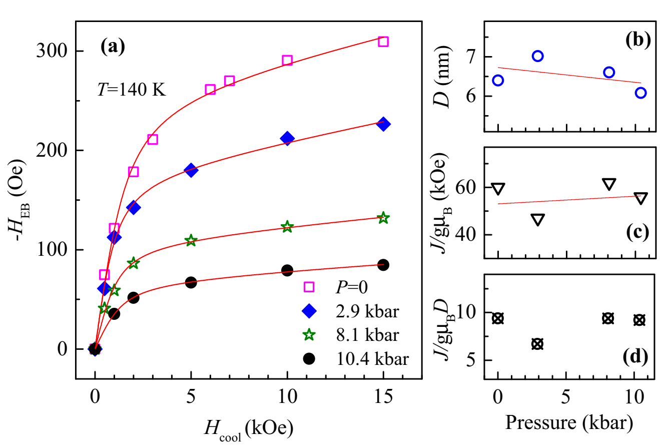

FIG. 5. (a) EB field H_{EB} as a function of cooling field H_{cool} at $T = 140\,\mathrm{K}$ at several pressures. Solid lines represent the best fits with Eq. (1). The FM cluster size D (b), interfacial exchange interaction $J/g\mu_{\mathrm{B}}$ (c), and ratio $J/g\mu_{\mathrm{B}}D$ (d) versus pressure.

Most likely, the coexisting FM and AFM nanoclusters, responsible for both GP and EB, reside randomly at the local lattice distortions caused by the mismatch between the sizes of the Gd and Sr ions. These deformed localities hold an expanded lattice and therefore hold Co states with higher spin (HS and IS states) and stronger Co-Co exchange interactions, allowing emergence of the FM and AFM phases in the system. Applied pressure compresses the lattice, effectively removing the local structure deformations through a well-known pressure-induced transition from HS state to the LS one. Such a spin-state conversion is preferable because the Co^{3+} ion size at LS state is much smaller than in the HS state. Likely, the applied pressure, through this spin-state transformation selectively removes the centers of quenched disorder represented by the FM and AFM ordered regions above T_C. The above analysis of CW behavior in $Gd_{0.5}Sr_{0.5}CoO_{3-\delta}$ shows that the average value of Co spin reduces from 1.065 to 0.903 under pressure of 10.4 kbar. Therefore, we assume that the mechanism of the variable spin state may be responsible for the pressure-induced decay of the Griffiths phase and the simultaneous exchange-bias collapse in this phase. We also note that due to this specific mechanism inherent in cobaltites, the Griffiths temperature T_G in $Gd_{0.5}Sr_{0.5}CoO_{3-\delta}$ speedily decreases with pressure with the coefficient $dT_G/dP = -3.6$ K/kbar. This contrasts strongly with the slight increase in T_G with pressure at a rate of $dT_G/dP \sim +0.16$ K/kbar found for the Dy_5Si_3Ge intermetallic compound [37].

In summary, we have shown that the applied hydrostatic pressure decreases T_C in $Gd_{0.5}Sr_{0.5}CoO_{3-\delta}$, in good agreement with the trend observed for cobaltites with a narrow bandwidth W. More interestingly, it was found that pressure strongly suppresses the Griffiths phase and the associated EB effect. The temperature T_G linearly decreases with pressure at a rate of $dT_G/dP = -3.6$ K/kbar, while the EB field at $T = 140$ K decreases by more than four times, and completely disappears at temperatures $T > 170$ K, at applied pressure of 10 kbar. Thus, the applied pressure modifies the magnetic phase diagram of $Gd_{0.5}Sr_{0.5}CoO_{3-\delta}$: the temperature region of paramagnetic phase expands and the regions of GP and FM phase contract. We assume that pressure effectively eliminates local structure deformations that are associated with the FM and AFM clusters above T_C and the well-known property of cobaltites to reduce the Co^{3+} spin under pressure plays an important role in this process.

[1] I. O. Troyanchuk, N. V. Kasper, D. D. Khalyavin, H. Szymczak, R. Szymczak, and M. Baran, Phys. Rev. Lett. **80**, 3380 (1998).
[2] P. G. Radaelli and S.-W. Cheong, Phys. Rev. B **66**, 094408 (2002).
[3] M. Kriener, C. Zobel, A. Reichl, J. Baier, M. Cwik, K. Berggold, H. Kierspel, O. Zabara, A. Freimuth, and T. Lorenz, Phys. Rev. B **69**, 094417 (2004).
[4] D. Phelan, Despina Louca, K. Kamazawa, M. F. Hundley, and K. Yamada, Phys. Rev. B **76**, 104111 (2007).
[5] M. A. Korotin, S. Yu. Ezhov, I. V. Solovyev, V. I. Anisimov, D. I. Khomskii, and G. A. Sawatzky, Phys. Rev. B **54**, 5309 (1996).
[6] P. L. Kuhns, M. J. R. Hoch, W. G. Moulton, A. P. Reyes, J. Wu, and C. Leighton, Phys. Rev. Lett. **91**, 127202 (2003).
[7] M. J. R. Hoch, P. L. Kuhns, W. G. Moulton, A. P. Reyes, J. Lu, J. Wu, and C. Leighton, Phys. Rev. B **70**, 174443 (2004).
[8] D. N. H. Nam, K. Jonason, P. Nordblad, N. V. Khiem, and N. X. Phuc, Phys. Rev. B **59**, 4189 (1999).
[9] W. H. Meiklejohn and C. P. Bean, Phys. Rev. **102**, 1413 (1956); **105**, 904 (1957).
[10] J. Nogues, J. Sort, V. Langlais, V. Skumryev, S. Surinach, J. S. Munoz, and M. D. Baro, Phys. Rep. **422**, 65 (2005).
[11] Y. K. Tang, Y. Sun, and Z. H. Cheng, Phys. Rev. B **73**, 174419 (2006).
[12] W. G. Huang, X. Q. Zhang, H. F. Du, R. F. Yang, Y. K. Tang, Y. Sun, and Z. H. Cheng, J. Phys.: Condens. Matter **20**, 445209 (2008).
[13] M. Patra, S. Majumdar, and S. Giri, J. Appl. Phys. **107**, 033912 (2010).
[14] I. Fita, R. Puzniak, A. Wisniewski, V. Markovich, I. O. Troyanchuk, and Yu. G. Pashkevich, J. Appl. Phys. **114**, 153910 (2013).
[15] R. B. Griffiths, Phys. Rev. Lett. **23**, 17 (1969).
[16] J. Deisenhofer, D. Braak, H.-A. Krug von Nidda, J. Hemberger, R. M. Eremina, V. A. Ivanshin, A. M. Balbashov, G. Jug, A. Loidl, T. Kimura, and Y. Tokura, Phys. Rev. Lett. **95**, 257202 (2005).
[17] S. M. Zhou, Y. Li, Y. Q. Guo, J. Y. Zhao, X. Cai, and L. Shi, J. Appl. Phys. **114**, 163903 (2013).
[18] C. He, M. A. Torija, J. Wu, J. W. Lynn, H. Zheng, J. F. Mitchell, and C. Leighton, Phys. Rev. B **76**, 014401 (2007).
[19] W. G. Huang, X. Q. Zhang, G. K. Li, Y. Sun, Q. A. Li, and Z. H. Cheng, Chin. Phys. B **18**, 5034 (2009).
[20] I. O. Troyanchuk, M. V. Bushinsky, and L. S. Lobanovsky, J. Appl. Phys. **114**, 213910 (2013).
[21] J. Yu, D. Louca, D. Phelan, K. Tomiyasu, K. Horigane, and K. Yamada, Phys. Rev. B **80**, 052402 (2009).
[22] I. Fita, I. O. Troyanchuk, T. Zajarniuk, P. Iwanowski, A. Wisniewski, and R. Puzniak, Phys. Rev. B **98**, 214445 (2018).
[23] S. M. Zhou, Y. Q. Guo, J. Y. Zhao, L. F. He, and L. Shi, Europhys. Lett. **98**, 57004 (2012).
[24] T. Vogt, J. A. Hriljac, N. C. Hyatt, and P. Woodward, Phys. Rev. B **67**, 140401(R) (2003).
[25] I. O. Troyanchuk, N. V. Kasper, D. D. Khalyavin, A. N. Chobot, G. M. Chobot, and H. Szymczak, J. Phys.: Condens. Matter **10**, 6381 (1998).
[26] M. Baran, V. Dyakonov, L. Gladczuk, G. Levchenko, S. Piechota, and H. Szymczak, Physica C **241**, 383 (1995).
[27] I. Fita, R. Szymczak, R. Puzniak, A. Wisniewski, I. O. Troyanchuk, D. V. Karpinsky, V. Markovich, and H. Szymczak, Phys. Rev. B **83**, 064414 (2011).
[28] J.-S Zhou, J.-Q. Yan, and J. B. Goodenough, Phys. Rev. B **71**, 220103(R) (2005).
[29] A. J. Bray, Phys. Rev. Lett. **59**, 586 (1987).
[30] M. B. Salamon, P. Lin, and S. H. Chun, Phys. Rev. Lett. **88**, 197203 (2002).
[31] E. F. Kneller and F. E. Luborsky, J. Appl. Phys. **34**, 656 (1963).
[32] S. Roy, I. Dubenko, D. D. Edorh, and N. Ali, J. Appl. Phys. **96**, 1202 (2004).

[33] I. Fita, V. Markovich, A. Wisniewski, D. Mogilyansky, R. Puzniak, P. Iwanowski, L. Meshi, L. Titelman, V. N. Varyukhin, and G. Gorodetsky, J. Appl. Phys. **108**, 063907 (2010).

[34] D. Niebieskikwiat and M. B. Salamon, Phys. Rev. B **72**, 174422 (2005).

[35] S. Giri, M. Patra, and S. Majumdar, J. Phys.: Condens. Matter **23**, 073201 (2011).

[36] F. Radu and H. Zabel, in Magnetic Heterostructures: Advances and Perspectives in Spinstructures and Spintransport, in *Springer Tracts in Modern Physics*, edited by H. Zabel and S. D. Bader (Springer-Verlag, Berlin, 2008), Vol. 227, pp. 97–184.

[37] N. Marcano, P. A. Algarabel, J. Rodríguez Fernández, C. Magén, L. Morellón, Niraj K. Singh, K. A. Gschneidner, Jr., V. K. Pecharsky, and M. R. Ibarra, Phys. Rev. B **88**, 214429 (2013).